Production of hydrogen and carbon nanofilaments using a novel reactor configuration: hydrodynamic study and experimental results

Abir Azara, Jasmin Blanchard, Faroudja Mohellebi, El Hadi Benyoussef, François Gitzhofer and Nicolas Abatzoglou

Abstract− A novel reactor configuration combining two beds, a central fluidized bed and an annular mobile bed, was designed for the production of hydrogen and carbon nanofilaments via dry reforming of gases produced from the pyrolysis of plastic waste. This combination allows for easy recovery of these nanomaterials and, since the mixture of catalyst and carbon formed is continuously fluidized, it prevents blockage.
Understanding the hydrodynamics is crucial for choosing the optimal operating conditions. Thus, a cold mock-up unit of the same size has been built and used. Since the gases produced by plastic pyrolysis are mainly composed of unsaturated hydrocarbons, the prototype reactor setup has been operated using ethylene as a surrogate molecule. The preliminary experimental results of the reactor operation with ethylene obtained so far are very promising and confirm the operability of the process. Next step is to operate continuously for longer time and reach a production of 1kg/h of carbon nanofilaments.

***Keywords*− Carbon nanofilaments, Fluidized bed, Hydrodynamics, Hydrogen, Reactor.**

NOMENCLATURE

CNF	Carbon Nanofilaments.
DR	Dry reforming
FBR	Fluidized bed reactor
FEG	Field emission gun
FCC	Fluid catalytic cracking
SBE	Spouted bed reactor
SEM	Scanning electron microscopy
TOS	Time-on-stream
XRD	X-Ray diffraction

I. INTRODUCTION

Various types of reactors are used for thermocatalytic reactions such as dry reforming (DR). The most conventional ones are: fixed bed [1–3], fluidized bed (FBR) [4–6], rotary [7–9] and membrane reactors [10–12]. Fixed bed reactors have several problems, and their use remains limited on a laboratory scale because it is easier at this scale to provide a high energy supply in order to overcome the endothermicity of DR reaction. Nevertheless, this heat transfer represents a major drawback at industrial scale and still remains a major techno-economic challenge for the large-scale industrial processes [13].
Fluidized bed reactor (FBR) is also widely studied [5]. This type of reactor promotes heat and mass exchange between the gas and catalyst particles, thus ensuring a good mass transfer and a nearly uniform temperature in the reactor. In addition, this type of configuration makes it easy to add and remove catalyst, allowing for easier process scale-up [14–17].
There are also membrane reactors which have been extensively studied in the literature and applied to reforming processes of hydrocarbons and oxygenated hydrocarbons [10,18–21]. The interest of this type of reactor consists in the selective separation of the hydrogen from the products in order to push the balance in the direction of the products and, thus, increase the yields. This is particularly interesting for industrial reforming because at the desired high pressure operation the conversion even at equilibrium is typically lower than 75%.
When it comes to produce carbon, the fixed bed also presents the risk of blockage due to the accumulation of carbon on the catalyst particles. In the case of fluidized beds, the friction between the catalyst particles allows the carbon to detach and be carried away with the gas. There are several types of FBR configurations, such as: fluid catalytic cracking FCC riser reactors, spouted bed reactors SBR [22] and SPR with a draft tube which are called also Wurster type FBR [23]. However, FBR also presents some drawbacks, such as the variation of the bed density, particles attrition and the rupture of carbon nanostructures are the main drawbacks [7,9].
Researchers have long wanted to improve conventional fluidized bed reactors to ensure and optimize the operability of the process at industrial scale, which has resulted in many innovative reactor configurations. For example, Bajad et al. [15] developed a new reactor configuration consisting of co-central compartments for the conversion of plastic waste into

Manuscript received August 31, 2022; revised December 3, 2022.

This work was supported by PRIMA Québec (grant R10-010) and the National Science & Engineering Research Council of Canada (grant CRDPJ 500331-16).

A. Azara from department of Chemical and Biotechnological Engineering, Université de Sherbrooke, Sherbrooke, CANADA and also from Laboratoire de Valorisation des Énergies Fossiles, École Nationale Polytechnique. (e-mail: abir.azara@usherbrooke.ca / abir.azara@g.enp.edu.dz).
J. Blanchard from KWI polymers, Canada (e-mail: jblanchard@kwipolymers.ca).
E.H Benyoussef and F.Mohellebi are from Laboratoire de Valorisation des Énergies Fossiles, École Nationale Polytechnique. (e-mails:Elhadi.benyoussef@g.enp.edu.dz, ferroudja.iddir@g.enp.edu.dz).
F. Gitzhofer and N. Abatzoglou are from department of chemical and Biotechnological Engineering, Université de Sherbrooke, Sherbrooke, CANADA (e-mails:François.gitzhofer@usherbrooke.ca, Nicolas.abatzoglou@usherbrooke.ca).

Digital Object Identifier (DOI): 10.53907/enpesj.v2i2.115

liquid hydrocarbons, carbon nanotubes and hydrogen-rich syngas (**Fig. 1**). The advantage of this configuration is that the heat has been provided in the annulus to heat both compartments and reduce the need for energy. The reactor presented in this work is also a novel configuration. It is a combination of a fixed bed and a moving bed. The advantage of this configuration is that it facilitates the recovery of CNF which is done mechanically during the fluidized bed phase.

Understanding the hydrodynamics of reactors with new configuration is important for choosing the optimal operating conditions for appropriate operation. Using a cold mock-up on Plexiglas is an efficient means to visualize the complex phenomena that occur between the gas phase and solid particles. It helps also when retrofit modifications to an existing reactor is required [24].

The purpose of this work is to present a comprehensive study of the reactor hydrodynamics and to present the proof of the scale-up process operability by presenting the first experimental results.

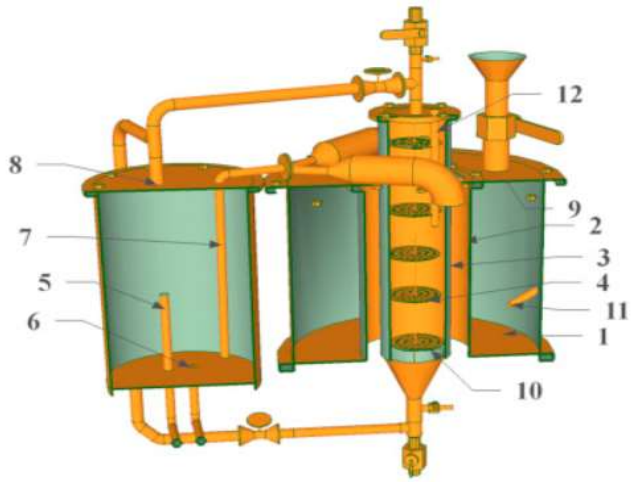

Fig. 1: Reactor cut section showing inner chambers and catalyst tray arrangement. (1 – pyrolysis chamber, 2 – heating chamber, 3 – CNT chamber, 4 – catalyst tray, 5 – oil drain line, 6 – water drain line, 7 – pyrolysis gas line to condenser, 8–non condensable gases to CNT chamber, 9 – Plastic feeder, 10 – first tray, 11 & 12 – thermo well) [15].

II. Cold Mock-up and Hydrodynamic Study

A. *Experimental set-up*

The prototype of a plexiglass reactor, used in this study to analyze the behavior of the gas phase and the solid phase inside the reactor, is presented in **Fig. *2*Erreur ! Source du renvoi introuvable.** and the dimensions are presented in **Erreur ! Source du renvoi introuvable.**. it is composed of two concentric cylinders, two lateral outlets and a conical base. The gas enters from the bottom through a distribution grid to ensure a uniform supply and exits through one of the two side outlets, the other outlet being closed. A grid is also located at the outlet to prevent the catalyst from being carried outside, however allowing the gas to exit freely.

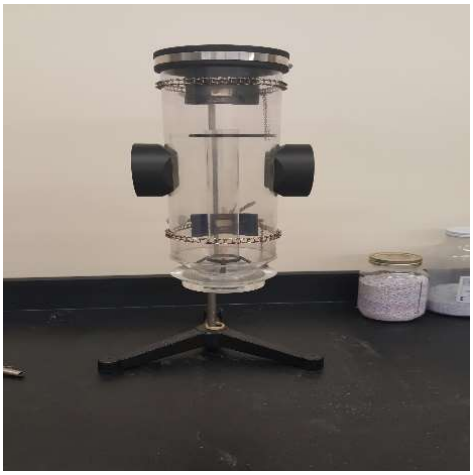

Fig. 2 : Reactor mock-up.

Table I
Prototype dimensions

External cylinder diameter (cm)	12
Internal cylinder diameter (cm)	3.8
Entrance diameter (cm)	3.8
Exit diameter (cm)	4
External cylinder height (cm)	38
Internal cylinder height (cm)	27
Wall thickness (cm)	0.16
Angle of the conic base	45 °

B. *Experimental conditions*

The study of the pressure drop of the bed as a function of the superficial gas velocity is the conventional method which can give an idea of the fluidization regime.

The compressed air from the main line first passes through a mass flow meter (0-100 LPM), then passes through the pipe towards the reactor inlet; the gas flow is distributed using a perforated plate located at the reactor inlet. The outlet is linked to a pipe which is connected to the vacuum. The reactor has two gauges to measure the pressure at the top and bottom and therefore calculate the pressure drop. The two pressure sensors are connected to the computer via two acquisition cards. The pressure measurements are read directly on the screen. Particles of 300 microns and density equal to 1657 kg/m^3 were used as solid phase. A graduated scale was stuck at the external surface to measure the height of the reactor.

C. *Results and Discussion*

There are three different regions in the reactor (**Fig. 3**): the spout (S), the annulus (A) and the fountain (F).

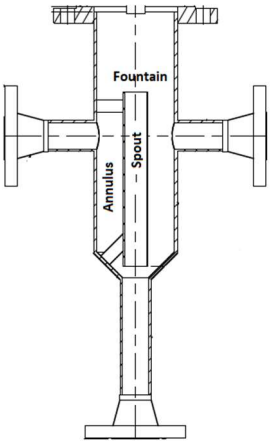

Fig. 3: Different regions in the reactor.

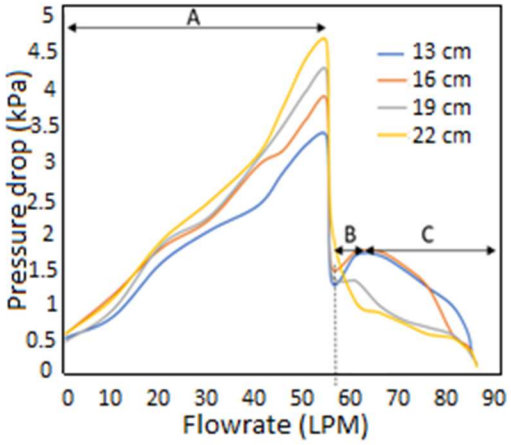

Fig. 5 : Pressure profile.

First, the movement of the catalyst was observed by visually following the profile over time of a layer of the same material but of a different color which was deposited at the surface of the bed in the annular section before the beginning of the tests. We observed that the movement of the solid is circular. The gas has two ways to reach the outlets: (a) by passing through the catalytic bed in the annular section towards the two outlets or (b) continue vertically to the end of the inner cylinder and then change direction towards the two outlets. If the gas flow is high enough along the entire length of the inner cylinder, the solid particles are fluidized (spout region S) and spring out like a fountain (fountain region F). In parallel with this movement, the solid particles in the annular region fall into the part below the inner cylinder to be entrained again allowing a slow downward movement of the catalyst in the annular part (region A). The latter, as shown in **Fig. 4** has been clearly proven by the descent of the colored layer. Over time, the color of particles becomes homogenous; because the colored layer reaches the bottom, and it is fluidized too; this oscillatory movement finishes by homogenizing the fluidized granular material. Since one of the two outlets has been used in our runs, the descent on one side is faster than the other. In fact, at industrial scale this lack of symmetry can be remedied by collecting the outlet gas flow through a radially positioned grid into another external annular section.

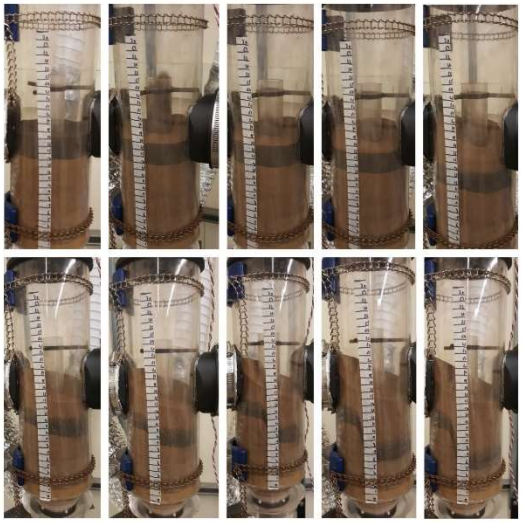

Fig. 4 : Visualization of catalyst movement.

The bed pressure drop was measured over fluidizing velocity in small steps for different solid heights. The results of the pressure drop profile (**Fig. 5**) corroborate with the visual observations. We observe the existing of three distinct zones:

Zone A: blocking period

We notice that the pressure drop increases with the flow rate for the four bed heights; and it is higher with a higher height (mass) of the bed. The explanation is that the catalyst particles that are below the inner cylinder block the flow of gas as long as the weight of the catalytic bed is higher than the pressure drop due to the flow through the bed. Thus, pressure drop increases over flow rate.

Zone B: explosion period

We notice that after the plug, the pressure drop drops suddenly, because the plug is pushed away.

13 and 16 cm: the pressure drop increases a little bit.

19 cm: the pressure drop remains constant.

22 cm: the pressure drop continues to fall with the same slope.

For this period, the pressure is high enough to burst the plug and its force exceeds the weight of the bed in the inner cylinder causing the bed to expand rapidly in the inner cylinder and the solids to spurt out. The net decrease is attributed to the fact that the mass of the fluidized material in the inner cylinder is lower during the operation in zone B than that during zone A conditions. In other words, the amount of the fluidized material expelled equals the amount of that re-entering the inner concentric tube and it is lower than the amount placed initially in the bed.

Zone C: recirculation period

13 and 16 cm: pressure drop remains constant for a while and then decreases.

19 cm: after the explosion period, pressure drop decreases directly for high flow rates.

22 cm: after the explosion period, pressure drop decreases with a slower slope when increasing the flow rate.

During this period, the solids of the annular region fall in the lower part of the inner cylinder to be fluidized and entrained which makes a periodic oscillatory movement of entrainment of the solids characterized by a slow downward movement of the bed in the annular part and an entrainment in the inner cylinder .

The minimum flow rate to pass from zone A to zone B is near 55 SLPM for nearly all heights tested.

III. Scale up process

A. Materials

The targeted feedstock is gases derived from plastic pyrolysis, which are largely composed of unsaturated HC. The initial step, which is presented in this work, is the use of ethylene as a surrogate molecule.

The catalyst used is Fe supported on alumina. Since the aim is to test the operation of the reactor, the use of a well-known catalyst was recommended.

B. P&ID

The set-up presented in **Fig. 6** is composed of three operation sections, the first one is reaction section, where the reaction is conducted in the novel reactor vessel (R1), covered by a heating jacket with temperature control. The catalyst is deposited inside the reactor and gases are fed from commercial gas cylinders (supplied by LINDE): C_2H_4 (99%), CO_2 (99%) and then preheated. Three ALICAT mass flow controllers were used to control the gas flows at the inlet. The CNF are removed from the catalyst due to the friction and entrained with the exiting gas to enter the filtration section where they are retrieved from the gas using metallic filters at an efficiency as high as approximately 90%. This filter is cleaned up periodically using N_2 pulsations and the CNF are collected in reservoir R2 in the recovery section. The filtration section and recovery sections are inside an appropriate designed space with negative pressure that is suitable for handling nanomaterials. The last section comprises the exchanger for the quenching of gaseous stream and the final conditioning through the glycol bath for the complete removal of water vapors prior to final disposal through a flameless and smokeless flare. The flow rate of the products is measured using a totalizer and its composition is analyzed by gas chromatography (Scion 400 Series GC).

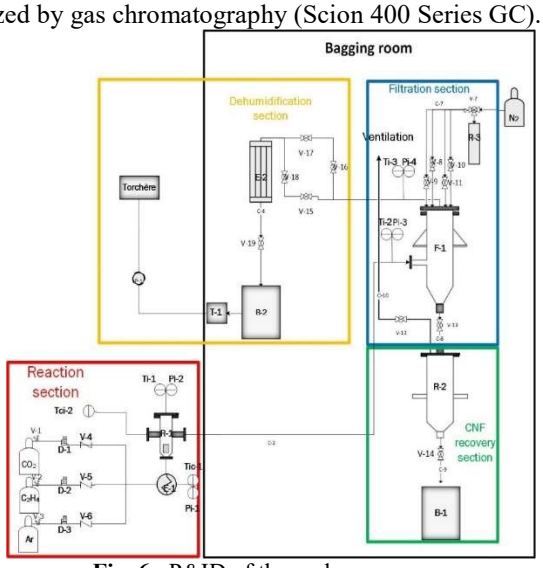

Fig. 6 : P&ID of the scale up process

C. Experimental methodology

Preparation of the catalyst

The catalyst used is Fe supported on alumina and it was prepared via wet impregnation. Iron nitrate ($Fe(NO_3)_3.9H_2O$) is dissolved in water (volume greater than pore volume) then the alumina is added. The mixture is stirred for 4 hours until it becomes a "slurry". The slurry is dried at 105°C overnight to remove remaining solvent. The catalyst is then calcined under an air atmosphere for 3 hours at 750 at 2° C./min. Finally, the catalyst is crushed and sieved down to 250 microns.

Activation of the catalyst

The catalyst was activated under a flow of 50% H_2 and 50% Ar for a time-on-stream (TOS) of 0.5 hour. **Table *II*** shows the activation test conditions.

Table II
Activation conditions

Catalyst	H_2 flow rate (SLPM)	N_2 flow rate (SLPM)	Catalyst Weight (kg)	TOS (h)	T(°C)
Fe/Al_2O_3 (10 wt%)	1	3	0.5	0.5	550

Reaction and CNF and H_2 production

CNF were produced via ethylene DR reaction. The reaction conditions are presented in **Table *III*.**

The reaction temperature was chosen following a study of thermodynamic equilibrium at temperatures ranging from 350 °C to 850 °C. The study is presented in the Results and Discussion section. Even though it was found in the hydrodynamic study that the minimum fluidization flow (transition from zone A to zone B) is approximately 55 SLPM, the total flow used is four SLPM. This is due to the high pressure generated by the very high flow rate feed, that the reactor is designed to operate at a pressure of 2.5 atm. On the other hand, to ensure the detachment of the carbon from the catalyst particles, pulses were made every 10 minutes using nitrogen to fluidize the bed for two minutes.

Table III
Reaction conditions

Catalyst	C_2H_4 flow rate (S LPM)	CO_2 flow rate (S LPM)	Catalyst Weight (kg)	TOS (h)	T(°C)
Fe/Al_2O_3 (10 wt%)	3	1	0.5	6	600

Characterization techniques

Two techniques were used to characterize the catalysts and carbon produced:

X-Ray diffraction (XRD) analysis was used to identify the catalyst crystalline structure before and after reaction. The diffractograph used is Philips X'pert PRO equipped with a Cu tube as its X-ray source and a Ni filter which is used to only let through Kα1 radiations from Cu (1.5418 Å) produced at 40 kV and 50 mA. The anti-dispersion slit was set at 1/2 and the divergence slit at 1/4. The analysis is carried out with a scanning angle 2θ ranging from 15 to 90°.

Scanning electron microscopy (SEM) was used to characterize the carbons formed and to study their morphology. The microscope used is a S-4700 Hitachi with field emission gun (FEG). It is equipped with detectors for secondary electrons (SE) and backscattered electrons (BSE). the working distance is 2.5-12mm and the accelerating voltage ranges from 1kV to 30kV. The magnification is up to 200,000X with resolution down to 5nm.

Reaction metrics

The extent of the reaction is evaluated by calculating: C_2H_4 conversions ($X_{C_2H_4}$), H_2 yield (Y_{H_2}) and carbon yield (Y_C).

$$X_{C_2H_4}\ (\%) = \frac{(F_{C2H4,in} - F_{C2H4,out})}{F_{C2H4,in}}$$

$$Y_{H_2}\ (\%) = \frac{F_{H2}}{2 \times F_{C2H4,in}} \times 100$$

$$Y_C\ (\%) = \frac{m_{C\ deposit}}{m_{C,in}} \times 100$$

$m_{C_{deposit}} = m_{catalyst,tf} - m_{catalyst,t0}$

$m_{C,in} = ((2 \times F_{C2H4,in} \times \text{time} + F_{CO2,in} \times \text{time})) * M_C$

Where:

$F_{C2H4,in}$ and $F_{C2H4,out}$ respectively denote the molar flow rates of C_2H_4 at the inlet and the outlet of the reactor,

F_{H2} the molar flow rate of H_2 at the outlet of the reactor,

$m_{C,in}$ the mass of carbon fed,

$m_{c\,deposit}$ the mass of solid carbon deposit on the catalyst,

$m_{catalyst,tf}$ the mass of the catalyst after reaction,

$m_{catalyst,t0}$ the mass of the catalyst before reaction,

M_C the molar mass of C = 12.0107 g.mol^{-1}.

D. Results and Discussion

Thermodynamic investigation

FactSage software was used to study the thermodynamic equilibrium of the C_2H_4 DR reactions at different conditions of temperature (450-850 °C) and molar ratios C_2H_4/CO_2 (1/1-3/1), at atmospheric pressure. Equilibrium composition as well as the amount of deposited carbon were estimated. This investigation allowed us to choose the experimental conditions which optimize carbon and synthesis gas ($CO+H_2$) yields. The most useful results are shown in **Fig. 7** and **Fig. 8**.

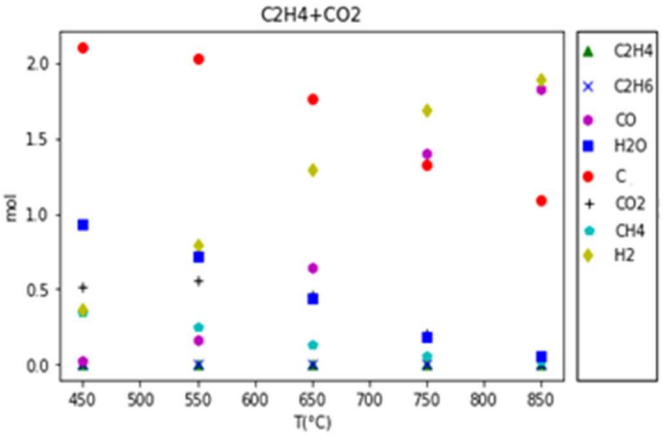

Fig. 7: Product composition for ethylene DR at ratio 1/1

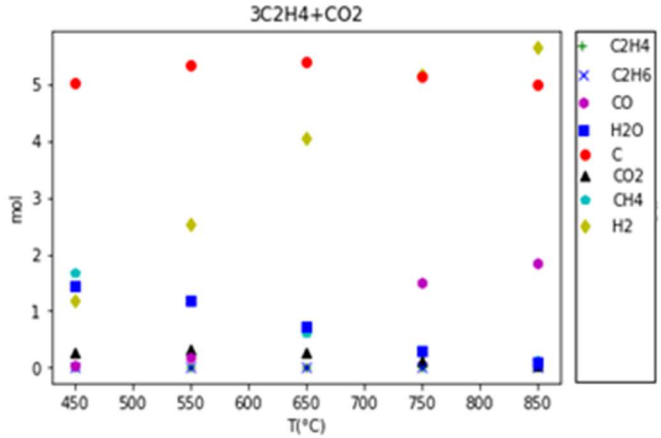

Fig. 8: Product composition for ethylene DR at ratio 3/1

We can observe that H_2 amount increases with temperature for both ratios, while C amount decreases with temperature at ratio 1/1; and reaches its maximum at temperature between 600-650 °C at a ratio of 3/1. Based on these results, 600 °C was chosen as the reaction temperature. Since we want to maximize carbon and H_2 production, a 3/1 ratio of C_2H_4/CO_2 was chosen.

Experimental results

The results of the reaction at 600 °C and ratio 3/1 are presented in **Table *IV***.

Table IV
General experimental results for the DR reaction at 600 °C and Fe-Al_2O_3 10% for 4h TOS.

C_2H_4 (SLPM)	3
CO_2 (SLPM)	1
Catalyst weight (kg)	0.5
TOS (hours)	6
$GHSV_{STP}$ (l.h^{-1}. kg^{-1})	480
C_2H_4/CO_2	3
Carbon (g)	615
Carbon growth rate ($kg_C.kg_{cat}^{-1}.h^{-1}$)	0.2
Carbon yield (%)	53.2
Total H_2 yield (%)	46.4
Total C_2H_4 conversion (%)	73.0
Total CO_2 conversion (%)	69.9
Mass balance error for C (%)	6.3
Mass balance error for H (%)	4.0
Mass balance error for O (%)	4.3

The carbon formed was analyzed by SEM and it has been proven that it is filamentous as shown in **Fig. 9**.

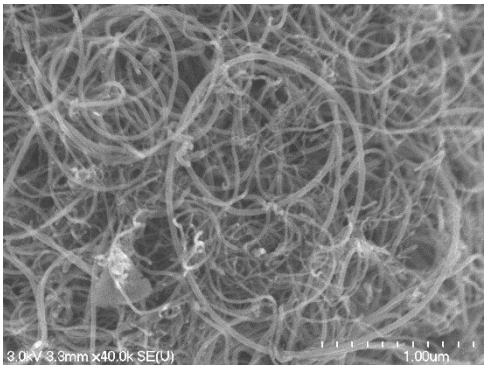

Fig. 9: SEM of deposited carbon

Fig. 10 and **Fig. 11** show the XRD of the fresh catalyst and deposited carbon on used catalyst after the DR reactions, respectively.

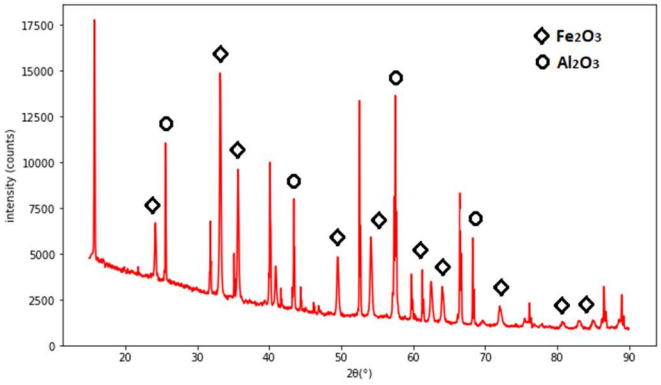

Fig. 10 : XRD of fresh catalyst

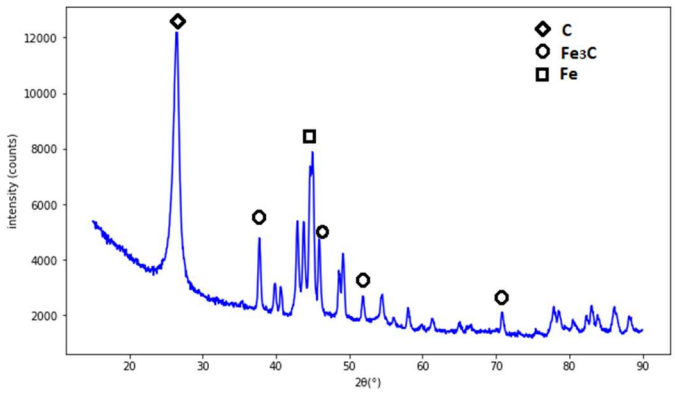

Fig. 11 : XRD of the spent catalyst

Discussion

The production of CNF at a pilot scale in a continuous mode has not been reported in the literature. In this work, we managed to operate a kilo lab scale reactor. The carbon produced in the reactor has been removed from the catalyst particles thanks to the friction between the particles which are in continuous movement between the two beds. The CNF with nanometric size were entrained with the existing gaseous stream and retrieved in the filter.

The carbon and H_2 yields are 53% and 46% respectively. These high rates are due to the suitable activity of the iron-based catalyst. Although the first reduction step with H_2 activated the catalyst, the H_2 formed at the beginning of the reaction contributes to catalyst activation by further reduction of iron oxides. This is proven by the presence of Fe metal peaks and the disappearance of iron oxide peaks on used catalyst XRD (**Fig. 11**). Also, carbon itself may contribute to the catalytic activity. It has been demonstrated that the carbon under the form of catalytically induced CNF itself has catalytic properties [25].

The XRD of used catalyst after the reaction, proves the deposition of carbon. The peak at 2θ=26° confirms that the carbon formed is graphitic. Moreover, no peaks of oxides have been found and only Fe was present in the diffractograms; the latter prove that Fe oxides were reduced during the reactions. Carbide formation was expected, because carbides are known to be the precursor of CNF especially with iron based catalyst; Fe_3C is metastable under the reaction conditions and it is decomposed to CNF and α-Fe [26]. Consequently, carbides co-exist along with CNF and Fe^0.

The SEM analyses reported above help us to identify the morphology of carbon produced. It is well known that there are different types of carbon that can be produced, pyrolytic, encapsulating and filamentous. Filamentous carbon is formed from the catalytic decomposition of HC, pyrolytic carbon is formed from HC thermal decomposition at high T, and encapsulating carbon is usually formed at relatively low T when the adsorbed HC accumulate on the surface of the catalyst and the C_nH_m* radicals slowly polymerize [27]. **Fig. 9** shows clearly that the carbon formed is filamentous with different width and length.

IV. Conclusion

Compared with waste plastics, CNF and H_2 are high-added-value products. Many efforts have been deployed to produce them at industrial scale with an optimized process in terms of energy efficiency, continuity and the facility of the system operation. This work is part of such an endeavor. The reactor conceived, built and operated is a novel configuration which has several advantages: especially in terms of recovery of carbon nanofilaments.

The process development unit used in this study is at pilot kg-lab scale, with the use of half a kg of catalyst and a total flow rate of reactants of four SLPM. Even though some problems occurred, the system worked very well, and more than 600 g of carbon was produced. The main drawback is that the scale is still low and after some hours of operation, there is a tendency of carbon accumulation at the relatively small orifices. Nevertheless, this study proved the concept at nearly kg-lab scale and further improvement will come along with a bigger scale up which is the intention of the research and industrial partner for the next steps towards commercialization.

Acknowledgment

The authors are indebted to PRIMA Québec (grand R10-010), the National Science & Engineering Research Council of Canada (grand CRDPJ 500331-16), as well as the companies KWI Polymers Solutions Inc. and Soleno Inc. for funding related to this project.

References

[1] A.H. Fakeeha, A.A. Ibrahim, W.U. Khan, K. Seshan, R.L. Al Otaibi, A.S. Al-Fatesh, Hydrogen production via catalytic methane decomposition over alumina supported iron catalyst, Arab. J. Chem. 11 (2018) 405–414. https://doi.org/10.1016/j.arabjc.2016.06.012.

[2] Y. Binhang, Y. Xiaofang, W. Jie, Y. Siyy, M. MyatNeoZin, G. Elaine, X. Zhenhua, K. Shyam, X. Wenquian, C. Jingguang G., Dry Reforming of Ethane and Butane with CO2 over PtNi/CeO2 Bimetallic Catalysts, ACS Catal 6 11 7283-7292. (2016).

[3] A. Drif, N. Bion, R. Brahmi, S. Ojala, L. Pirault-Roy, E. Turpeinen, P.K. Seelam, R.L. Keiski, F. Epron, Study of the dry reforming of methane and ethanol using Rh catalysts supported on doped alumina, Appl. Catal. Gen. 504 (2015) 576–584. https://doi.org/10.1016/j.apcata.2015.02.019.

[4] J.L. Pinilla, M.J. Lázaro, I. Suelves, R. Moliner, J.M. Palacios, Characterization of nanofibrous carbon produced at pilot-scale in a fluidized bed reactor by methane decomposition, Chem. Eng. J. 156 (2010) 170–176. https://doi.org/10.1016/j.cej.2009.10.032.

[5] J.L. Pinilla, R. Moliner, I. Suelves, M.J. Lázaro, Y. Echegoyen, J.M. Palacios, Production of hydrogen and carbon nanofibers by thermal decomposition of methane using metal catalysts in a fluidized bed reactor, Int. J. Hydrog. Energy. 32 (2007) 4821–4829. https://doi.org/10.1016/j.ijhydene.2007.08.013.

[6] P. Ugarte, P. Durán, J. Lasobras, J. Soler, M. Menéndez, J. Herguido, Dry reforming of biogas in fluidized bed: Process intensification, Int. J. Hydrog. Energy. 42 (2017) 13589–13597. https://doi.org/10.1016/j.ijhydene.2016.12.124.

[7] J.L. Pinilla, R. Utrilla, M.J. Lázaro, I. Suelves, R. Moliner, J. M. Palacios, A novel rotary reactor configuration for simultaneous production of hydrogen and carbon nanofibers, Int. J. Hydrog. Energy. 34 (2009) 8016–8022. https://doi.org/10.1016/j.ijhydene.2009.07.057.

[8] J.L. Pinilla, R. Utrilla, M.J. Lázaro, R. Moliner, I. Suelves, A.B. García, Ni- and Fe-based catalysts for hydrogen and carbon nanofilament production by catalytic decomposition of methane in a rotary bed reactor, Fuel Process. Technol. 92 (2011) 1480–1488. https://doi.org/10.1016/j.fuproc.2011.03.009.

[9] S.L. Pirard, A. Delafosse, D. Toye, J.-P. Pirard, Modeling of a continuous rotary reactor for carbon nanotube synthesis by catalytic chemical vapor deposition: Influence of heat exchanges and temperature profile, Chem. Eng. J. 232 (2013) 488–494. https://doi.org/10.1016/j.cej.2013.07.077.

[10] A.V. Alexandrov, N.N. Gavrilova, V.R. Kislov, V.V. Skudin, Comparison of membrane and conventional reactors under dry methane reforming conditions, Pet. Chem. 57 (2017) 804–812. https://doi.org/10.1134/S0965544117090031.

[11] J. Múnera, S. Irusta, L. Cornaglia, E. Lombardo, CO2 reforming of methane as a source of hydrogen using a membrane reactor, Appl. Catal. Gen. 245 (2003) 383–395. https://doi.org/10.1016/S0926-860X(02)00640-3.

[12] Improved hydrogen production from dry reforming reaction using a catalytic packed-bed membrane reactor with Ni-based catalyst and dense PdAgCu alloy membrane - ScienceDirect, (n.d.). https://www.sciencedirect.com/science/article/pii/S036031991530692 3?via%3Dihub (accessed May 11, 2018).

[13] R. Aiello, J. E Fiscus, H.-C. Zur Loye, M. D Amiridis, Hydrogen production via the direct cracking of methane over Ni/SiO2: Catalyst

deactivation and regeneration, Appl. Catal. Gen. 192 (2000) 227–234. https://doi.org/10.1016/S0926-860X(99)00345-2.
[14] I. Barbarias, G. Lopez, M. Artetxe, A. Arregi, J. Bilbao, M. Olazar, Valorisation of different waste plastics by pyrolysis and in-line catalytic steam reforming for hydrogen production, Energy Convers. Manag. 156 (2018) 575–584. https://doi.org/10.1016/j.enconman.2017.11.048.
[15] G.S. Bajad, R.P. Vijayakumar, A.G. Gupta, V. Jagtap, Y. pal Singh, Production of liquid hydrocarbons, carbon nanotubes and hydrogen rich gases from waste plastic in a multi-core reactor, J. Anal. Appl. Pyrolysis. 125 (2017) 83–90. https://doi.org/10.1016/j.jaap.2017.04.016.
[16] A. Azara, S. Belbessai, N. Abatzoglou, A review of filamentous carbon nanomaterial synthesis via catalytic conversion of waste plastic pyrolysis products, J. Environ. Chem. Eng. 10 (2022) 107049. https://doi.org/10.1016/j.jece.2021.107049.
[17] R.-X. Yang, K.-H. Chuang, M.-Y. Wey, Effects of Nickel Species on Ni/Al2O3 Catalysts in Carbon Nanotube and Hydrogen Production by Waste Plastic Gasification: Bench- and Pilot-Scale Tests, Energy Fuels. 29 (2015) 8178–8187. https://doi.org/10.1021/acs.energyfuels.5b01866.
[18] K. El, S. Da, D. Ja, P. Wd, M. Le, C. Jgg, B. Dj, The role of rhenium in the conversion of glycerol to synthesis gas over carbon supported platinum-rhenium catalysts, J. Catal. 260 (2008) 164–177.
[19] H.R. Godini, S. Xiao, M. Kim, O. Görke, S. Song, G. Wozny, Dual-membrane reactor for methane oxidative coupling and dry methane reforming: Reactor integration and process intensification, Chem. Eng. Process. Process Intensif. 74 (2013) 153–164. https://doi.org/10.1016/j.cep.2013.09.007.
[20] B. Lee, S. Lee, H. Lim, Numerical modeling studies for a methane dry reforming in a membrane reactor, J. Nat. Gas Sci. Eng. 34 (2016) 1251–1261. https://doi.org/10.1016/j.jngse.2016.08.019.
[21] S. Sumrunronnasak, S. Tantayanon, S. Kiatgamolchai, T. Sukonket, Improved hydrogen production from dry reforming reaction using a catalytic packed-bed membrane reactor with Ni-based catalyst and dense PdAgCu alloy membrane, Int. J. Hydrog. Energy. 41 (2016) 2621–2630. https://doi.org/10.1016/j.ijhydene.2015.10.129.
[22] F.J. Weinberg, T.G. Bartleet, F.B. Carleton, P. Rimbotti, J.H. Brophy, R.P. Manning, Partial oxidation of fuel-rich mixtures in a spouted bed combustor, Combust. Flame. 72 (1988) 235–239. https://doi.org/10.1016/0010-2180(88)90124-1.
[23] D.E. Wurster, Particle coating process, US3253944A, 1966. https://patents.google.com/patent/US3253944A/en (accessed March 15, 2020).
[24] S. Sundaresan, Role of hydrodynamics on chemical reactor performance, Curr. Opin. Chem. Eng. 2 (2013) 325–330. https://doi.org/10.1016/j.coche.2013.06.003.
[25] S. Jankhah, N. Abatzoglou, F. Gitzhofer, J. Blanchard, H. Oudghiri-Hassani, Catalytic properties of carbon nano-filaments produced by iron-catalysed reforming of ethanol, Chem. Eng. J. 139 (2008) 532–539. https://doi.org/10.1016/j.cej.2007.08.031.
[26] M.A. Ermakova, D.Y. Ermakov, A.L. Chuvilin, G.G. Kuvshinov, Decomposition of Methane over Iron Catalysts at the Range of Moderate Temperatures: The Influence of Structure of the Catalytic Systems and the Reaction Conditions on the Yield of Carbon and Morphology of Carbon Filaments, J. Catal. 201 (2001) 183–197. https://doi.org/10.1006/jcat.2001.3243.
[27] A.-C. Dupuis, The catalyst in the CCVD of carbon nanotubes—a review, Prog. Mater. Sci. 50 (2005) 929–961. https://doi.org/10.1016/j.pmatsci.2005.04.003.

ABIR AZARA is an engineer and a holder of Master 2 in chemical engineering; she has graduated from Ecole Nationale Polytechnqiue of Algiers in 2016. Since 2017, she is a PhD candidate in Sherbrooke University in Canada. Her project is a synergistic work between the university and two industrial partners. It focuses on the production of carbon nanostructures using a gas produced from waste plastic pyrolysis. She has published so far three articles and has participated on several conferences across Canada and worldwide.

Jasmin Blanchard is Chief Technology Officer at KWI Polymers located in Boisbriand, Canada. He has a master and a PhD degree in chemical engineering from Sherbrooke University in Canada completed in 2005 and 2014 respectively. The PhD is a project on Fischer-Tropsch synthesis using a catalyst generated by plasma. His field of expertise include methane reforming, carbon nanofiber synthesis, pyrolysis of plastic, synthesis of black carbon by plasma and graphene synthesis by plasma.

Faroudja Mohellebi is Professor at the department of chemical engineering of the Ecole Nationale Polytechnique, Algiers, Algeria and was head of department of chemical engineering from February 2009 to December 2021. Professor Mohellebi works on the mobility and bioavailability of traditional contaminants like cadmium and nickel and on compounds of emerging interest like drugs. Her work focuses on analyzing contaminants, their chemical speciation, environmental fate and potential impacts. She has participated in the training of many students and has proposed many research topics directly related to the depollution of water loaded with emerging products and pesticides. She has numerous collaborations and projects at national and international level. Her scientific production includes publications, reviews, keynotes, and three book chapters.

El Hadi Benyoussef is professor at the department of chemical engineering of the Ecole Nationale Polytechnique, Algiers, and head of the laboratory 'laboratoire de valorisation des energies fossils LAVALEF'.

François Gitzhofer is full professor at the Department of Chemical & Biotechnological Engineering of the Université de Sherbrooke since 1991. He also served as Vice-Dean of Academic Affairs as well as Secretary of the Faculty of Engineering at the University of Sherbrooke. His main research contributions are related to materials synthesis including catalysts using Suspension Plasma Technology He is the co-applicant with professor Abatzoglou on the grant which funded this study.

Nicolas Abatzoglou is Professor and ex-Head of the Department of Chemical & Biotechnological Engineering of the Université de Sherbrooke. He is Adjunct Professor at the University of Saskatchewan and Fellow of the Canadian Academy of Engineering. He is a specialist in *Process Engineering involving particulate systems in reactive and non-reactive environments*. He is the Director of the GRTP (Group of Research on Technologies and Processes). The GRTP operates a brand new R&D and Scale-up facility at the Université de Sherbrooke and is financed by both Canadian & Quebec institutional funding and industrial partners such as Rio Tinto Iron & Titane, KWI and Soleno. From May 2008 to March 2021, he has been the holder of the Pfizer Industrial Research Chair in Pharmaceutical Processes. The highly successful output of this Chair led to a continuation of this association, which is now focusing on Process intensification, Analytical Technologies development and industrial applications. He has numerous collaborations and projects at national and international level and he served as one of the Leaders in Canada's NCE Network BioFuelNet on Biorefining. He is presently the Leader of the Canadian side of the project GOLD funded by HORIZON 2020 and comprising 18 partners from EU, China and Canada. He is co-founder of the company *Enerkem Technologies*, precursor of Enerkem, a spin-off commercializing technologies in the field of energy from renewable resources. He has received many academic and professional awards and he is a world-renowned researcher and technology transfer expert. His scientific production includes 200+ publications, reviews, conferences, keynotes, plenaries and invited lectures, patents and three book chapters.